Possible effects of Mercury surface temperatures on the exosphere

E. Rognini[1,2], A. Mura[3], M. T. Capria[3], A. Milillo[3], A. Zinzi[4], V. Galluzzi[3]

[1]ASI Space Science Data Center (SSDC), Via del Politecnico, 00133 Rome, Italy; [2]INAF-OAR Osservatorio Astronomico di Roma, Via Frascati 33, 00078, Monte Porzio Catone (RM), Italy
[3]INAF-IAPS Istituto di Astrofisica e Planetologia Spaziali, Via del Fosso del Cavaliere 100, 00133 Rome, Italy; [4]Agenzia Spaziale Italiana (ASI), Via del Politecnico snc, 00133, Rome, Italy

Introduction

The MESSENGER mission observed the characteristics of sodium exosphere of Mercury; an equatorial exospheric sodium emission [1] characterized by an enhancement above the cold-pole longitudes (so called because of their lower-than-average temperature) has been detected (fig. 1). The enhancement in sodium emission follows the cold pole dayside local time from dawn to dusk (fig. 2), in contrast with the models that predict a general enhancement only in the morning side due to the fast release of sodium atoms accumulated during the night when it rise in the sun light. This is a signature of the effect of surface temperature and thermal capacity and their influence on the surface release of volatile material. This has been confirmed by the data set obtained by ground based observation of THEMIS solar telescope [2] (fig. 3). We want to study the link between the surface temperature variations and the exosphere sodium content.

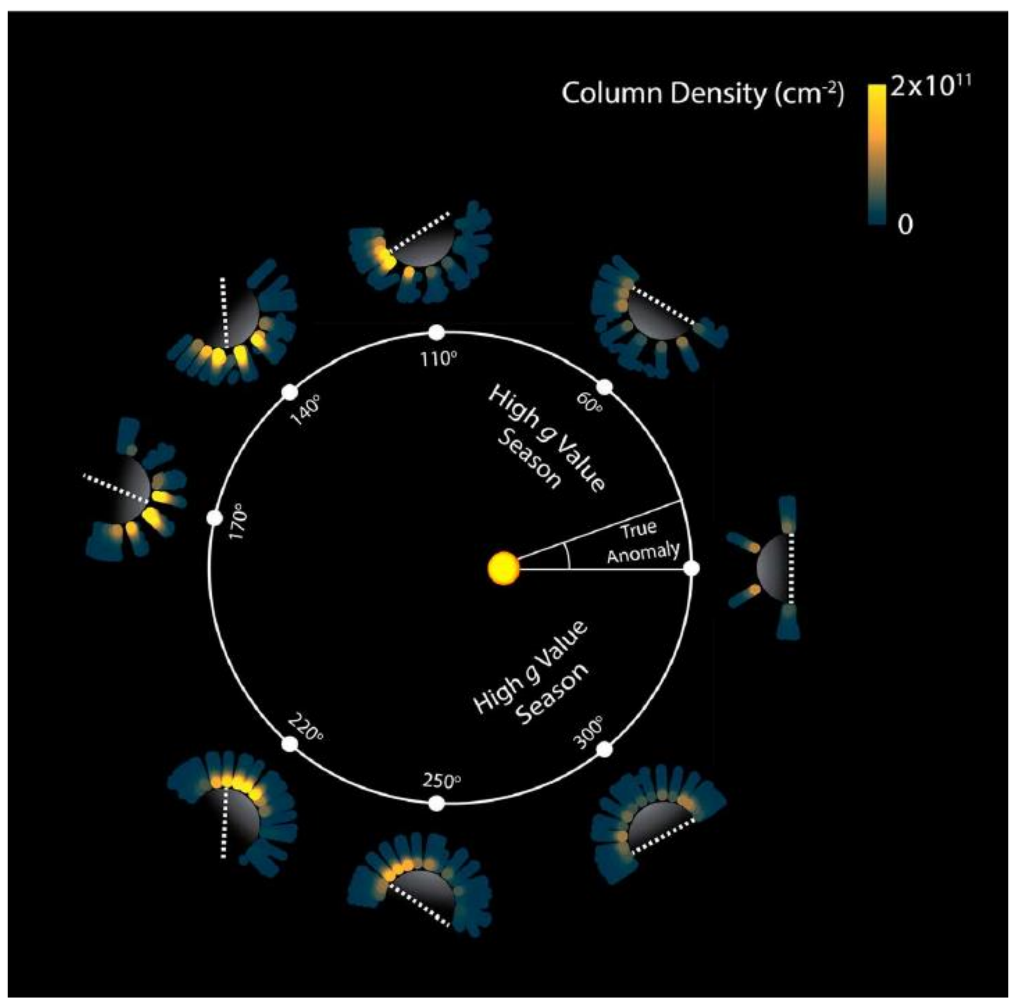

Figure 1. Observed sodium column density projected in the equatorial plane, as function of orbital phase. Figure from [1].

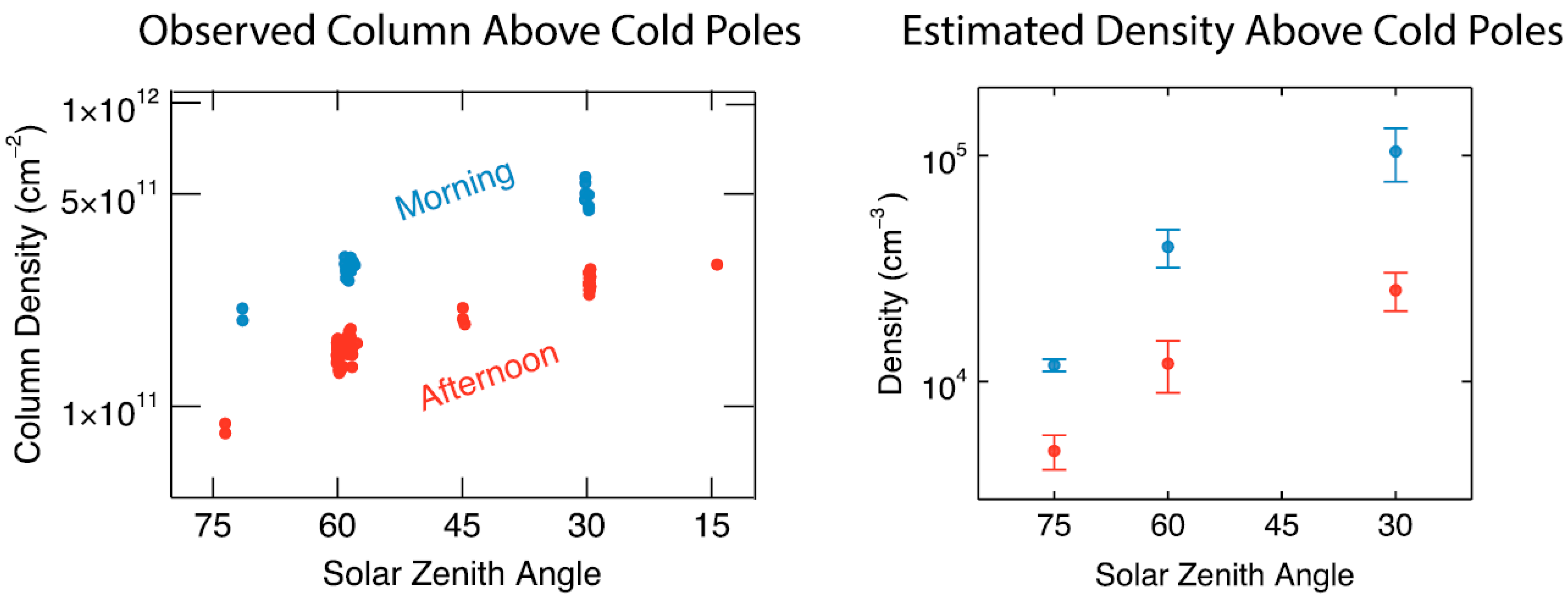

Figure 2. Comparison between observed and estimated sodium column density as function of solar zenit angle at the cold pole longitudes (±10 degrees). Figure from [1].

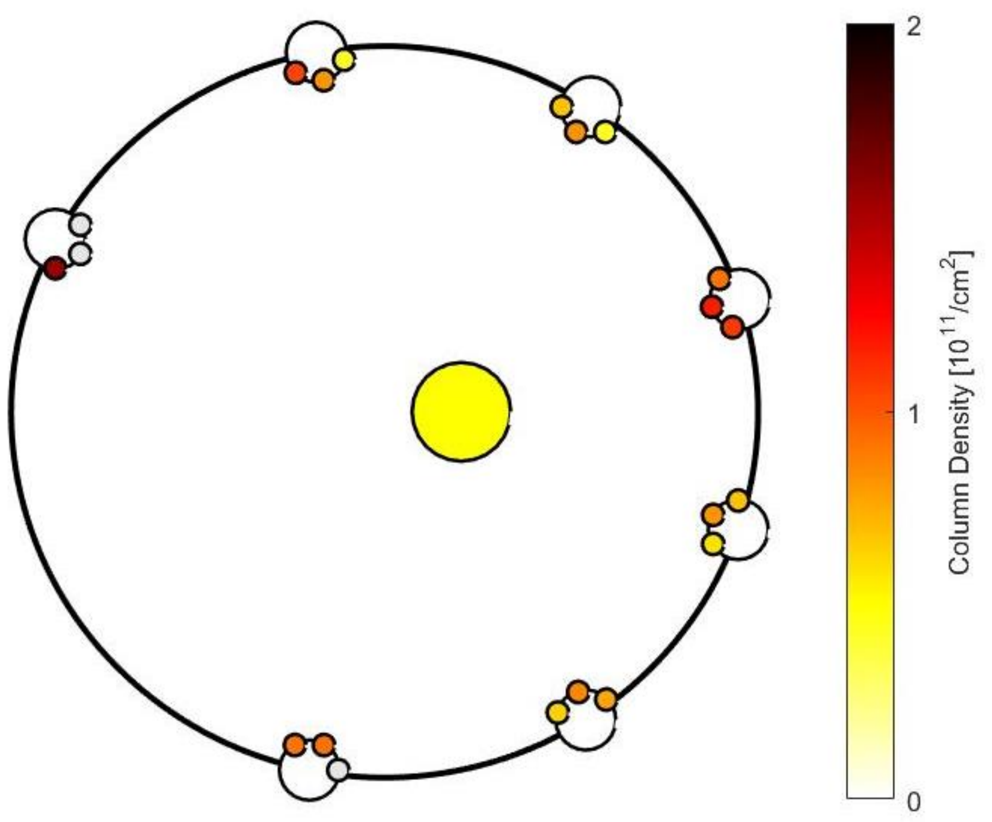

Figure 3. Schematic view of the equatorial LT asymmetries of the Na column density along the Mercury's orbit obtained from the THEMIS data set. Grey bullets represents no data available.

Methods

We study the link between the surface temperature and the sodium emission with the help of two different models linked together: a thermophysical model that calculates the surface temperature [3], and an exosphere circulation model [4]. The first one gives the temperature as function of thermal conductivity of the first cm of soil for each point on the surface; we can simulate different classes of material from fine dust to bedrock (in ascending order of thermal conductivity). The temperature distribution is the input for a 3D circulation model that calculates the sodium abundance and circulation in the exosphere.

Results

The calculated total exosphere sodium content is different from that resulting from a "temperature reference model" (temperature proportional to $\cos(\alpha)^{1/4}$ where α is the illumination angle). In fig. 4 we show the sodium total contents from the reference model function of time over one Mercury year (blue line) and the same quantity from the new thermophysical model (red line). An anticorrelation is present in the central part of the plot. The sodium content is the sum of two different processes: Photon Stimulated Desorption (PSD) and thermal desorption (TD). The sodium particles ejected in the exosphere by the TD have velocities much lower than the escape velocity and they fall down onto the surface; the PSD process is then dominant at high altitude (fig. 5).

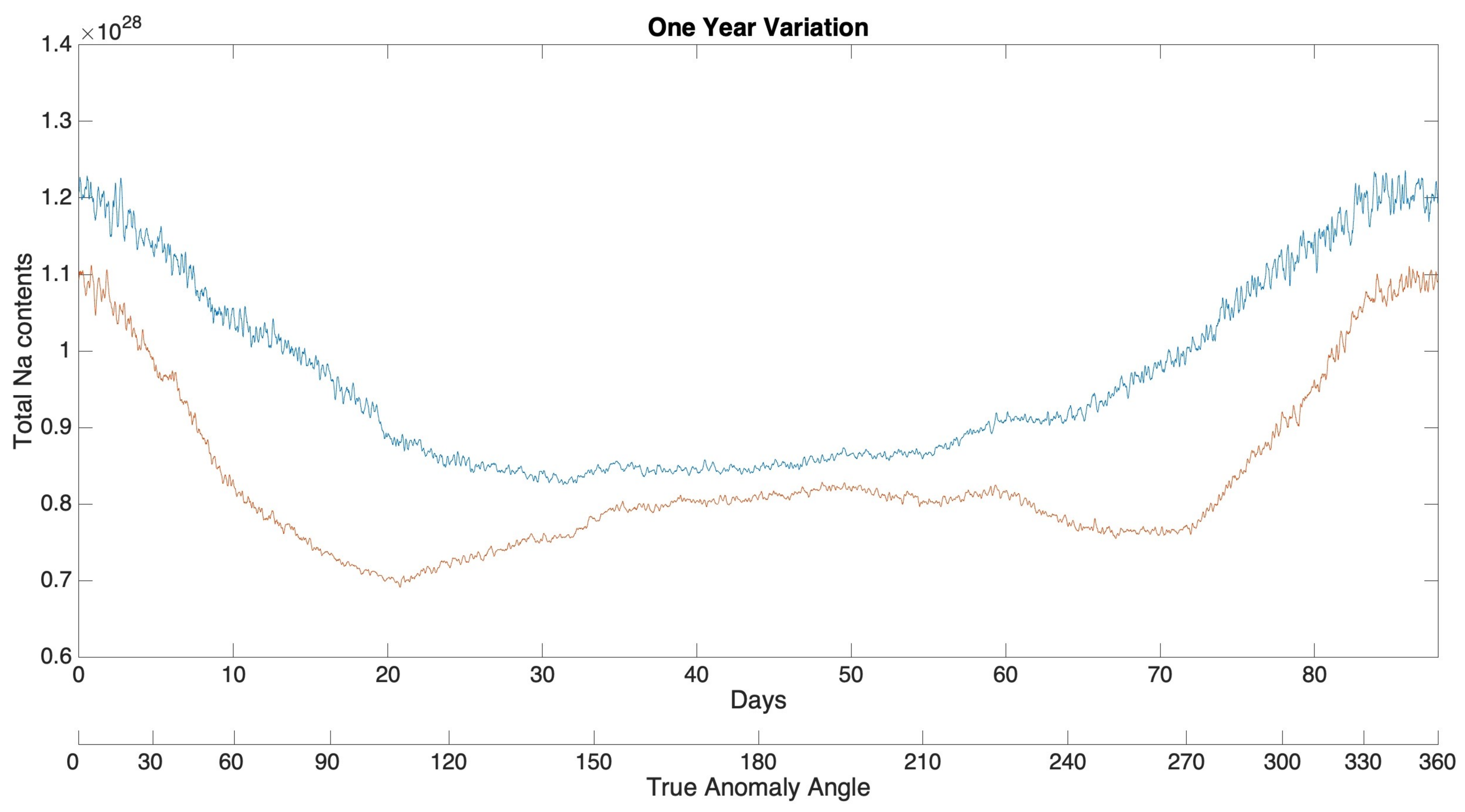

Figure 4. Total exosphere sodium content calculated by assuming a reference temperature (blue line) and the temperature calculated with the termophysical model (red line).

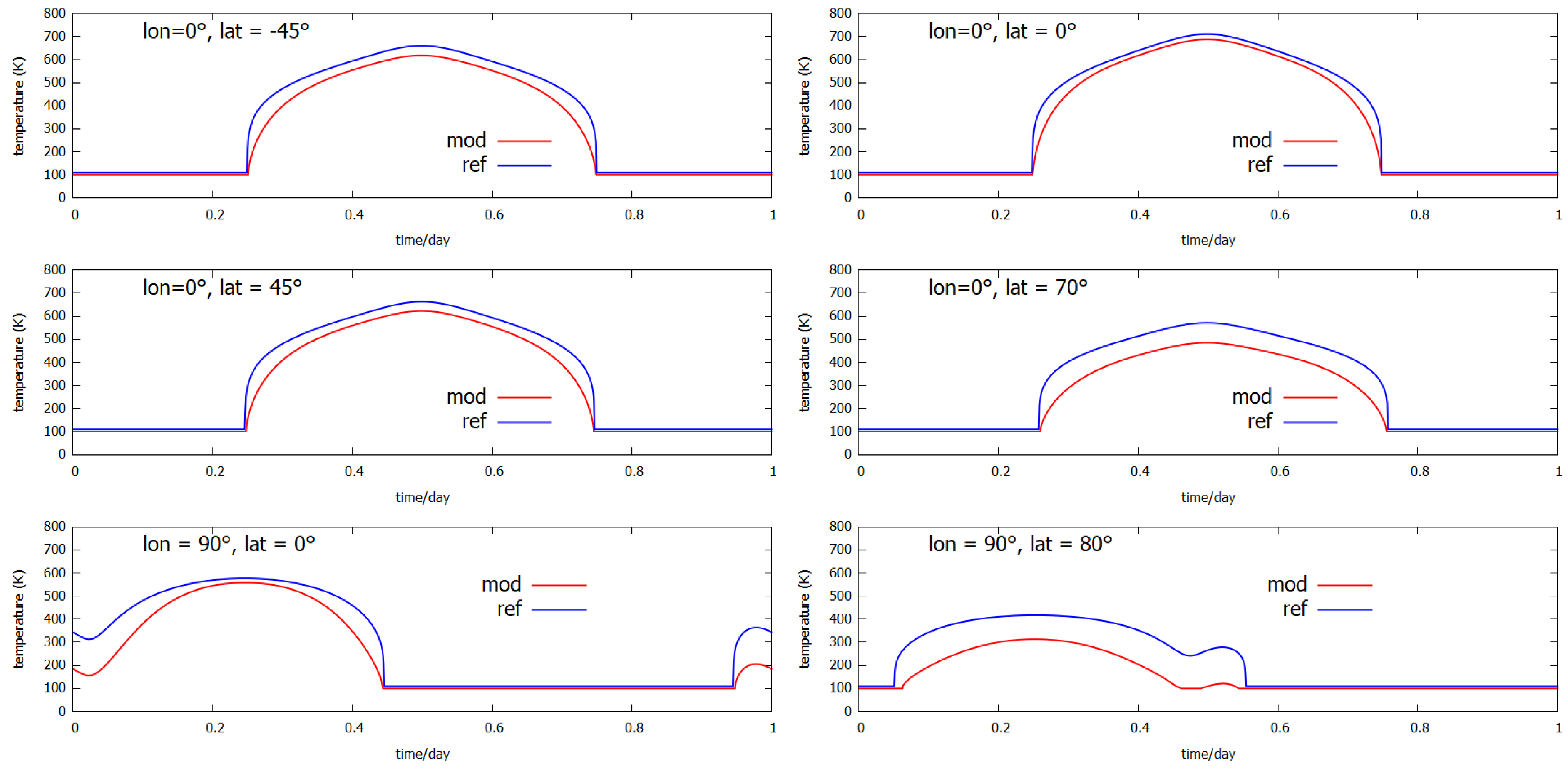

Fig. 5. Temperature as function of time (normalized to solar hermean day, 176 terrestrial days) for different locations (longitude-latitude points), calculated with the thermophysical code (red line) and with the reference temperature law (T proportional to ¼ power of illumination angle cosine, blue line). The local temperature rises (bottom plots) are due to temporary retrograde motion of the Sun, because the planet is at the aphelion and the angular orbital velocity is greater than the spin angular velocity.

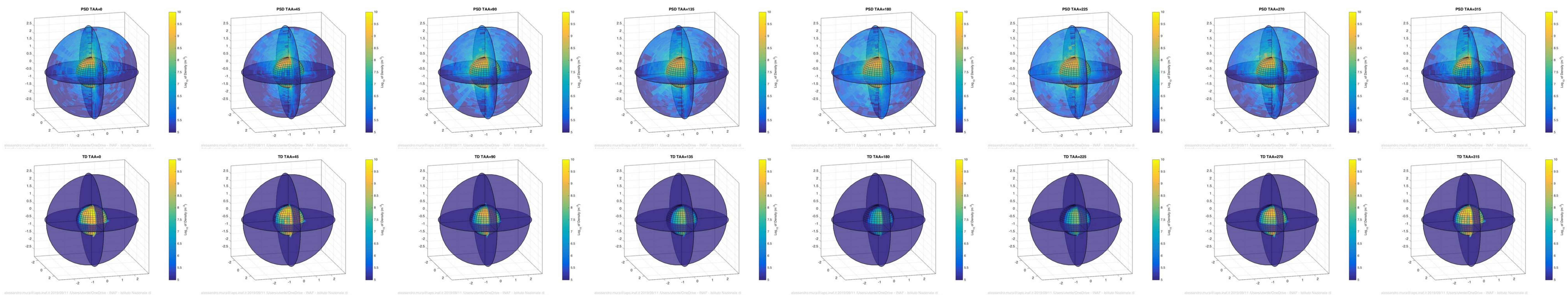

Figure 6. Results from the model of Mura et al., 2009. Each figure shows the simulated exosphere sodium density, plotted over 3 perpendicular planes and at the lowest altitude (i.e. just above Mercury surface), for a different value of true anomaly angle (degrees), and for the two processes of emission considered in the model: Photon Stimulated Desorption (PSD) and Thermal Desorption (TD). In the model, the emission of sodium is regulated by its abundance in the uppermost surface layer (which is calculated by the model at each iteration). The model includes the precipitation of plasma (which enhances the diffusion of sodium from the inside to the outside of the regolith grains), the circulation of exospheric sodium, the radiation pressure acceleration (variable with time, and maximum around 60 and 300° of TAA), photoionization of sodium, ion sputtering (not shown here), the rotation of the surface (including the short period of retrograde apparent motion close to perihelion), etc.

Conclusions

1. Different surface temperatures affect the calculated exosphere sodium.
2. It will be possible to compare the new data from the BepiColombo mission [5] with the results of the simulations.

A version of the thermophysical code is almost ready to be available to the scientific community through MATISSE [6], the webtool developed at the SSDC in ASI.

Acknowledgments. The computational resources used in this research have been supplied by INAF-IAPS through the DataWell project.

References.
[1] Cassidy, T. A., et al., A cold-pole enhancement in Mercury's sodium exosphere, Geophysical Research Letters, 43, 11, 2016.
[2] Milillo, A., et al. (2020), Exospheric Na distributions along the Mercury orbit with the THEMIS telescope, submitted to Icarus
[3] Rognini, E., et al. (2019), High Thermal Inertia Zones on Ceres From Dawn Data, JGR Planets, https://doi.org/10.1029/2018JE005733
[4] Mura, A., et al., The sodium exosphere of Mercury: Comparison between observations during Mercury's transit and model results, Icarus, Elsevier, 200, 2009.
[5] Benkhoff, J., American Geophysical Union, Fall Meeting, abstract #P23F-3501, 2018.
[6] Zinzi, A., et al. (2016), Astronomy & Computing, 15, 16-28